UNIVERSITY OF PLOVDIV
"PAISII HILENDARSKI"

FACULTY OF PHYSICS AND TECHNOLOGY
DEPARTMENT OF ELECTRONICS, COMMUNICATIONS
AND INFORMATION TECHNOLOGIES

Svetoslav Genchev Hadzhigenchev

GEOELECTRICAL RESISTIVITY TELEMETRY SYSTEM IN SEISMOGENIC ZONES

ABSTRACT

of a dissertation for a degree in science and education

"DOCTOR"

Field of higher education: 5. Technical sciences

Professional direction: 5.3. Communication and computer technology

Ph.D.:
Automation of areas of non-material sphere
(medicine, education, science, administration, etc.)

Supervisor:
Assoc. Prof. Dr. Slavi Yasenov Lyubomirov

Plovdiv, 2023

The dissertation has 166 pages, including 86 figures and 5 tables, organized in an introduction, 4 chapters, general conclusions, scientific and applied contributions, a list of terms and abbreviations used, and a list of the author's publications. The list of cited literature includes 105 titles.

The notations of the formulas, figures and tables in the abstract coincide with those in the thesis.

The dissertation was discussed and directed for defense at a meeting of the Departmental Council of the Department of "Electronics, Communications and Information Technologies" at Plovdiv University "Paisii Hilendarski" on 15.12.2023, Protocol No. 58/15.12.2023.

The defense of the dissertation will take place on 06.03.2024 at 11:00 a.m. in hall "BIL 15", Kostaki Peev 21 str. of Plovdiv University "Paisii Hilendarski" at a meeting of the scientific jury.

The materials for the doctoral defense are available to those interested in the office of the Faculty of Physics and Technology at the Paisii Hilendarski University of Plovdiv, Kostaki Peev 21 str., floor 4, room 1.

Scientific jury: Prof. Dr. Dimitar Mihaylov Tokmakov
Assoc. Prof. Dr. Daniela Antonova Shehova
Prof. Dr. Nedyalko Todorov Katranzhiev
Assoc. Prof. Dr. Borislav Hristov Milenkov
Assoc. Prof. Dr. Veselin Gerov Nachev

Author: Svetoslav Genchev Hadzhigenchev
Title: **GEOELECTRICAL RESISTIVITY TELEMETRY SYSTEM IN SEISMOGENIC ZONES**

Print run: 30 copies

GENERAL CHARACTERISTICS OF THE DISSERTATION

Relevance of the problem

The topic of this dissertation is related to the research in the field of earthquake prediction and, more specifically, to the monitoring of one of the well-established predictive effects - the change in the electrical resistivity of the Earth's crust in the process of earthquake preparation.

The physical processes occurring in a focal area before and during an earthquake manifest themselves in various physical phenomena that can be observed and measured at the Earth's surface. These include changes in the seismic wave velocities, the Earth's magnetic field, the Earth's electrical resistivity and electrothermal potentials, groundwater levels, radon concentration in hydrothermal wells, etc.

In some countries, over the years, particular attention has been paid to field recordings of these phenomena in relation to earthquake preparation. At the same time, where possible, laboratory measurements have been made and theoretical models of the observed phenomena have been built. The overall objective of these studies is to build a coherent theory (model) of the earthquake preparation and realization process that could explain the observed phenomena and provide a basis for their prediction.

Unfortunately, this goal has not been achieved yet.

One of the reasons for this is insufficient data – lack of or sparsely located monitoring stations, not covering the main fault scours. Furthermore, in accordance with Gutenberg-Richter law, the stronger earthquakes (with $M>5$) that we are interested in occur less frequently, i.e., long-term observations with reliable instrumentation are needed in seismogenic zones.

In terms of the new tectonic plate model, the territory of Bulgaria belongs to the southern parts of the Eurasian plate. The geodynamics of the region is mainly determined by the subduction of the African Plate in the Aegean Arc area and the collision of the Arabian Plate with the Eurasian Plate. Seismologically, it is part of the Alpo-Himalayan seismic belt and is subject to the effects of both local and neighbouring earthquakes. In the first 30 years of the 20th century alone, four earthquakes of magnitude $M \geq 7$ occurred in Bulgaria.

However, the work of monitoring and analysing the anomalies of the geophysical fields preceding earthquakes remains in the background. Systematic research in this direction is lacking. There are no established precursor observation areas - polygons. Taking into account the relevance and importance of the problem that generate the need to search for new methods and approaches to carry out in-depth field studies with data accumulation and processing, our attention was focused on the use of modern means for the implementation of a system of geoelectric resistivity telemetry in seismogenic zones.

The improvement of the instrumentation networks connected to modern communication networks is a necessary condition for the successful development of seismic protection measurements and earthquake prediction.

Objective of the dissertation work

The aim of the dissertation work is to develop a system for telemetry of geoelectrical resistivity and other earthquake precursors in seismogenic zones.

Tasks to achieve the goal:

1. To study the results of the research on the changes of geoelectrical resistivity and the existing methods and means of its measurement, carried out in order to establish their relationship with earthquakes.

2. To select an appropriate method and design an apparatus for measuring the variations of the geoelectrical resistivity. To simulate the operation of the main blocks with integrated design and analysis environments. To develop a method for calibration and verification of the apparatus. To investigate the influence of noises on the measurement results.

3. To carry out a hardware implementation of an apparatus for measuring the variations of the geoelectrical resistance. To develop measurement management software and install the equipment in field conditions.

4. To implement a system for transmission, processing and visualization of data from geoelectrical and other measurements. To develop software for the initial processing of the received data.

Research methods and tools used:

Existing methods, techniques and tools in the field of recording geoelectric resistivity changes in relation to earthquake preparation are investigated and systematized. Possible sources of noise and ways to reduce them are analysed.

Implementation and practical applicability

An apparatus for measuring variations in geoelectrical resistivity was designed, implemented and installed. The data obtained from the registration of geoelectrical resistivity and meteorological parameters for an eight-month period are shown. The software enables the registration, transmission, processing, storage and visualization of the received data on a cloud platform.

Publications on the topic

Independent: 3 publications in USB (Union of Scientists of Bulgaria) - Plovdiv, 1 publication in USB - Smolyan.

Co-authored with the supervisor: 1 publication in a National scientific conference with international participation - Smolyan.

Volume and structure of the dissertation

The dissertation is 166 pages long, including 86 figures and 5 tables arranged in an introduction, 4 chapters, general conclusions, scientific and applied contributions, a list of terms and abbreviations used, a list of the author's publications and a list of the literature cited.

CONTENTS OF THE DISSERTATION

CHAPTER I. RESULTS FROM THE LITERATURE REVIEW ON THE DISSERTATION TOPIC

1.1 Classifications of earthquake precursors and the place of apparent geoelectric resistivity variations in them

By their nature, the variations in apparent electrical resistivity are assigned to geophysical electrical precursors, along with the vertical electrical gradient of the atmosphere, geopotentials, natural electromagnetic fields, etc. In terms of the time of manifestation, they are in the group of medium-term type B precursors (when there is no relation of the precursor time to the earthquake magnitude).

1.2. The Bulgarian experience in earthquake monitoring and prediction

In this paragraph, the experimental and methodological work on earthquake precursor monitoring conducted in Bulgaria is reviewed:

- Measurements of radon concentration in the water of the Sofia mineral bath;
- Measurements of earth electric potentials at the seismic observatory "Vitosha" and seismic station "Krupnik". Interesting results were obtained and presented below;
- Measurement of helium concentration in a borehole near Simitli. No preceding anomalies were observed, but some coseismic correlation was found;
- Extensiometric devices at the same place that support the previous measurements;
- Radon at Krupnik seismic station. No correlation was found between radon concentration and earthquakes;
- Radon in three Bulgarian caves - "Bacho Kiro", "Sueva's Hole" and "Lepenitsa". The observed microextensions and radon emissions in the caves and their relation to seismicity are not sufficient at the current stage of research to talk about earthquake prediction;
- Geomagnetic measurements in Panagyurishte and Sofia;
- Apparent electrical resistivity in the area of NAO "Rozhen" and in "Tasladzha" area, near the town of Strazhitsa. The measurements were carried out by the author.

1.3. Ambiguity of precursors

Predicting an earthquake must answer three questions - when, where and with what magnitude will the future earthquake occur, i.e. information about its time, location and magnitude. No predictor can reliably predict an earthquake. Sometimes the anomaly exists but no earthquake occurs and vice versa. This phenomenon is called "*precursor ambiguity*". Therefore, after many years of observations in a region, a set of the most informative precursors is selected and monitored. So-called "polygons" are built for this purpose.

1.4. Nature of the earth's electrical resistivity and its anomalies

The factors determining the conductivity of the crust and the changes in its electrical resistivity before rocks breaking under compression in laboratory experiments are discussed.

1.5 Methods for measuring geoelectrical resistivity

The main methods of measuring the apparent resistivity with an artificial current source - the Wenner, Schlumberger and Dipole-Dipole methods - are described and compared.

1.6 Noises and methods to reduce their influence.

The factors that can affect the measured values of apparent resistivity by the methods described in the previous paragraph and ways to reduce them are discussed:

- Polarization of the receiving electrodes
- Telluric currents
- Presence of close conductors
- Current leakage
- Current induction in measuring cables
- Presence of industrial (stray) currents
- Seasonal variations of geoelectrical resistivity

1.7. Instrumentation for measuring geoelectrical resistance

The basic requirements for the apparatus are described. The advantages and disadvantages of existing solutions for measuring apparent resistivity are discussed.

1.8. Some results of observations of apparent resistivity variations in the process of earthquake preparation

Curves of apparent resistivity variations are shown in its observations in the Garm region, Tajikistan Republic of the former USSR, the San Andreas Fault region in the USA, Japan and China.

1.8.5 Observations in Bulgaria

Registration of anomalies of the earth's (apparent) electrical resistivity preceding the earthquakes in Bulgaria was conducted by the author with his own equipment in 1984-1985 near the seismic station in NAO "Rozhen" and after the earthquakes in the area of the town of Strazhitsa in 1987.

- *1984-1985, National Astronomical Observatory "Rozhen"*

Fig. 1.23. *Variations of apparent resistivity recorded by the author in the area of NAO "Rozhen"*

The author suggests that the observed variations in apparent resistivity are related to seismic activity. They can be caused by the preparation of relatively distant earthquakes - with epicentre up to about 250-300 km from the place of resistivity registration. The changes are a continuous decrease in resistance and begin to occur from a few hours to a little more than a day before the main shock. The amplitudes of the variations are from 10 to 30% - fig. 1.23.

- *1987, "Tasladja" area, Strazhitsa*

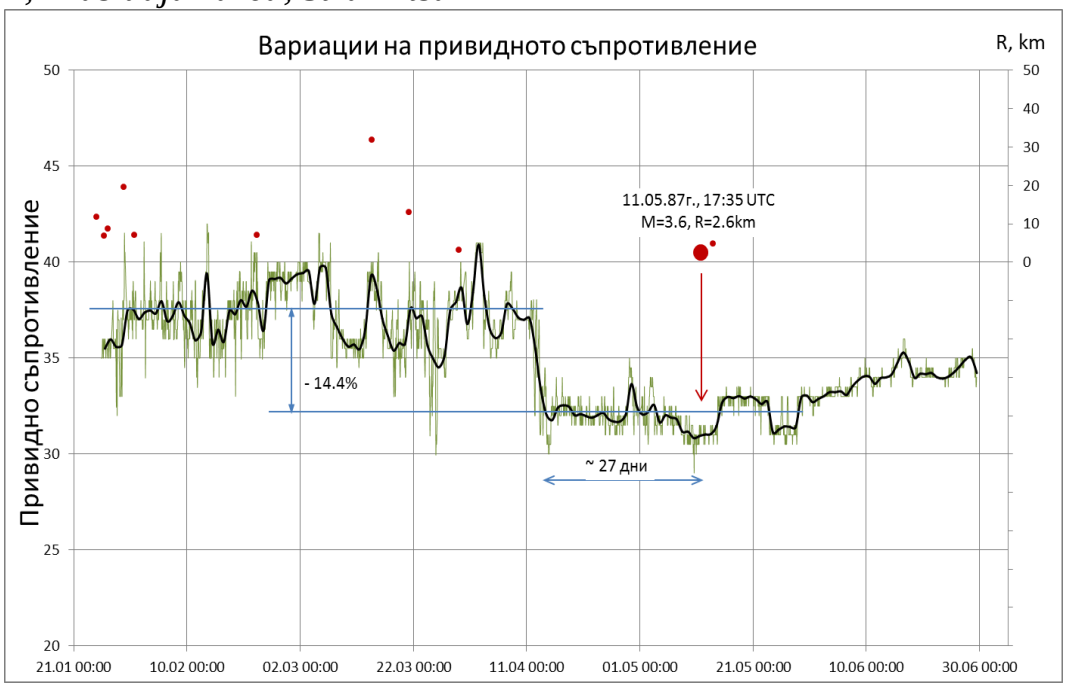

Fig. 1.24. *Variations of the apparent resistivity recorded by the author in the "Tasladzha" forest near the town of Strazhitsa*

In this case, the change is of the "bay" type with a continuous decrease in resistance, which according to most studies is the prevailing pattern. The change in average daily values

is -14.4%, and the lead time is about 4 weeks - fig. 1.24. Small red dots above the graph indicate weaker earthquakes, the magnitude of which is not available. The secondary vertical axis shows the epicentral distances to Strazhitsa station (STZ).

It is assumed that the observed changes in the apparent resistivity are related to the seismic activity because:

- The observed anomaly (~14.4%) of the apparent resistivity is 7 times larger than the standard deviation (~2%) before its onset and is therefore statistically significant.
- The moment of the minimum of the anomaly coincides with the moment of the earthquake.
- The pattern of the anomaly for the larger earthquake is similar to the pattern of the anomaly for the weaker earthquakes.

CHAPTER II. DESIGN OF APPARATUS FOR MEASURING VARIATIONS OF GEOELECTRICAL RESISTIVITY

In chapter two of the thesis, an apparatus for the measurement of the variations in geoelectrical resistivity is designed. A symmetrical Schlumberger circuit was chosen for its implementation because of the following advantages:

- the depth of investigation is greater compared to the Wenner scheme;
- it has high protection against stray industrial and telluric currents;
- lower power source requirements compared to dipole-dipole schemes;
- convenient for deployment in mountainous regions.

2.1 Electrodes and wires

2.1.1. Selection of the type of electrodes

To reduce the difference in polarization voltages, brass electrodes were chosen for the receivers and cheaper inox electrodes - for the supply electrodes. For the latter, the effect of electrode potentials is irrelevant.

2.1.2. Choice of electrode spacing

The choice of electrode spacing is closely related to the depth of the investigation. Achieving greater survey depths (effective probing depths, current line penetration) is necessary because of the following assumptions:

- Changes in the electrical resistivity of rocks caused by seismogenic sources are greater at greater depths.
- Changes in the electrical resistivity of the rocks due to disturbing sources (temperature, precipitation, atmospheric pressure, etc.) are smaller at greater depths. The depth of investigation should be greater than the depth of penetration of seasonal variations of the apparent resistivity.

To increase the depth of investigation, it is necessary to increase the distance between the A and B current electrodes. However, this leads to a decrease in the useful potential difference across the receiving electrodes M and N and a decrease in the signal-to-noise ratio. To prevent this from happening, it is necessary to increase the current strength in the power line, i.e. to use a more powerful source, thicker wires and batteries with higher capacity. All this leads to an increase in the cost of the installation.

Another limiting factor for increasing the distance between the current electrodes,

hence the depth of investigation, is the topography of the terrain. Finding a suitable location for the installation can be a difficult problem to solve, especially in mountainous areas. There it is difficult to find a relatively rectilinear site with greater spacing, except along gullies. Such installation has one advantage - the current electrodes are placed in a water-saturated environment and do not need to be watered during drought. The receiving electrodes are placed slightly outside the gully to avoid signal shunting during heavy rainfall.

Taking into account all these factors, the topography of the terrain and the experience gained so far, the length of the distance between electrodes A and B was chosen at 520 m, and that between electrodes M and N at 21.7 m. The geometric coefficient of the installation is calculated to 9770 (formula (3)).

The wires to the electrodes are of cable type LFC-79 (Light Field Cable) with 2 strands of braided copper and steel (2x0.35mm^2) connected in parallel.

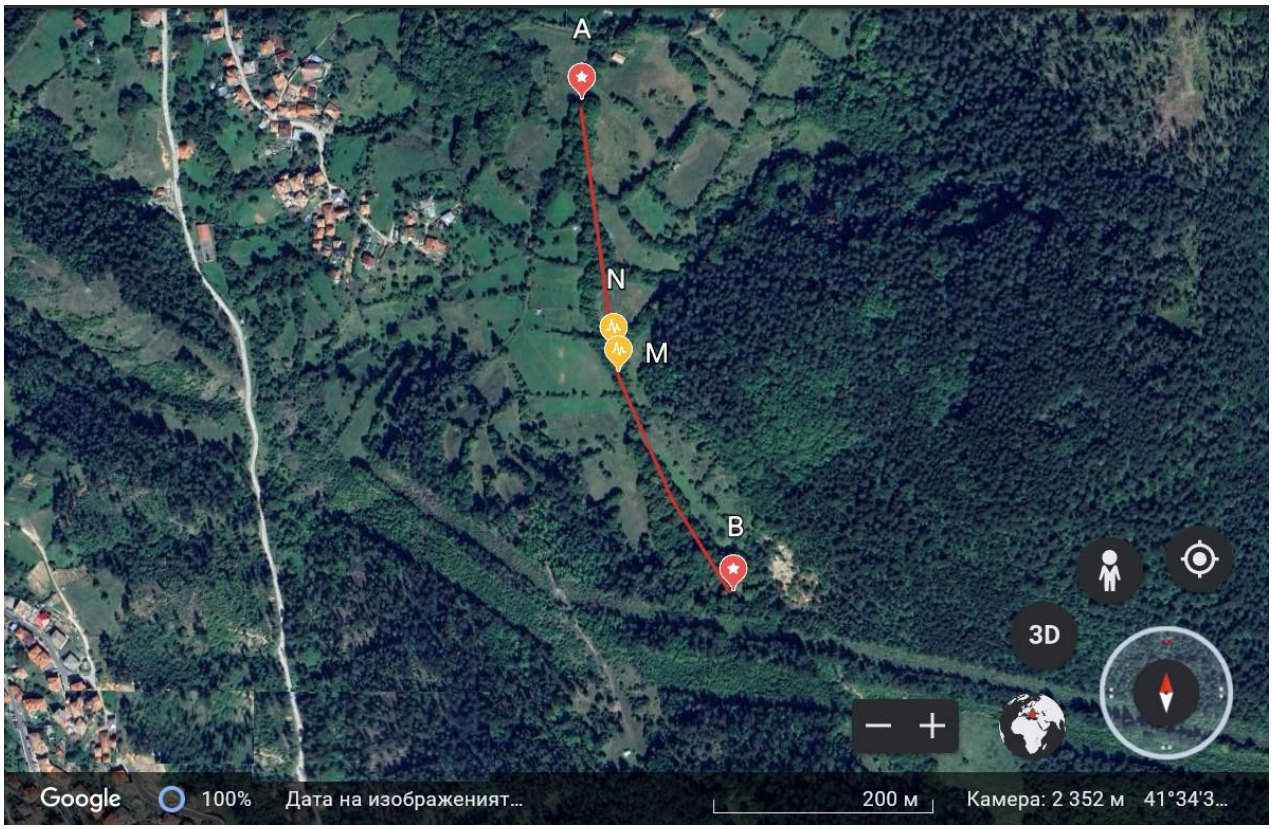

Fig. 2.1. *Selection of the installation site*

Fig. 2.1 shows the geographical location of the installation in the area of the village of Dunevo, Smolyan region. The site is located in one of the relatively weak seismic zones in the country - the Rhodope seismic zone.

2.2 Block diagram of the field part

Fig. 2.2 presents a block diagram of the field part of the designed apparatus, including the following blocks: ESP32 - central processing unit, RTC - real-time clock, SD card - SD card, AMPU - channel amplifier for voltage measurement, AMPI - channel amplifier for current measurement, H BRIDGE - H bridge, DC-DC - controllable inverter, I2C ADC, I2C DAC - ADC and DAC on I2C bus, LORA - LoRa modulation module, PM - power management module, TLP250 - optoisolators, ISO1540 - I2C bus isolators, HLK5D1212 - isolated DC-DC converters, Rain CPU - processor for measuring precipitation, Rain Gauge

- vessel for precipitation, ATH20 - module for measuring meteorological parameters, Ri - resistance for measuring current..

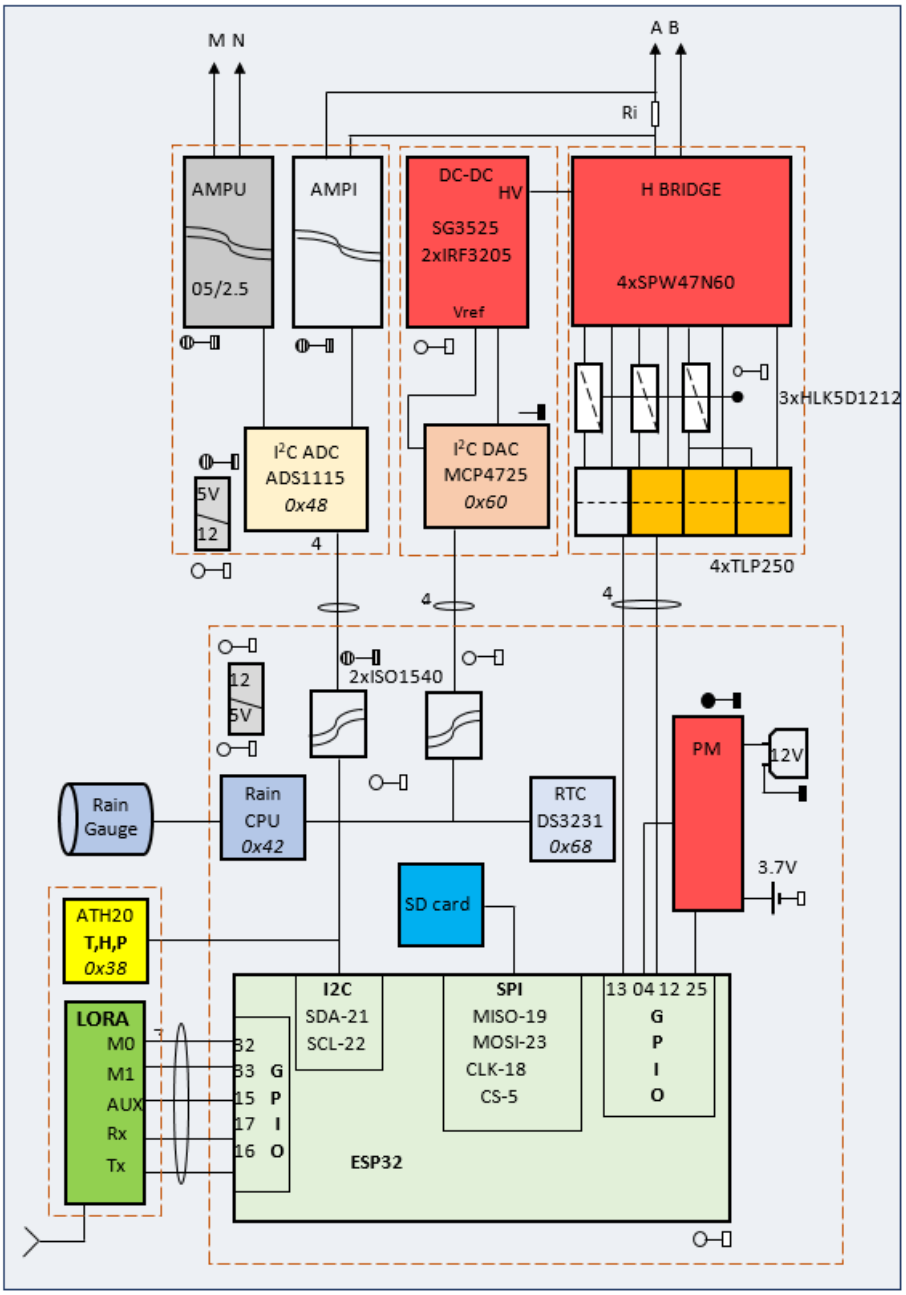

Fig. 2.2. *Block diagram*

2.3 Current source in the power line

The power line current source consists of a DC-DC converter and a power line current reversing circuit controlled by the microprocessor module and an optical splitting circuit.

The DC-DC converter is an isolated PUSH-PULL voltage inverter controlled by a PWM regulator SG3525. The duty cycle of the pulses at its outputs, and hence the current in the supply line, is varied by adjusting the voltage at pin 2 of the SG3525 (the non-inverting input of the difference amplifier). This voltage is set by an MCP4725 12-bit I2C digital-to-analog converter (I2C DAC) controlled by the microprocessor module using an ISO1540 isolated I2C bus.

To eliminate the interfering DC components of the input signal (mainly from the difference in polarization of the electrodes), the measurements of the input signal amplitude are made in the forward and reverse directions of the current in the supply electrodes - Fig. 2.3.

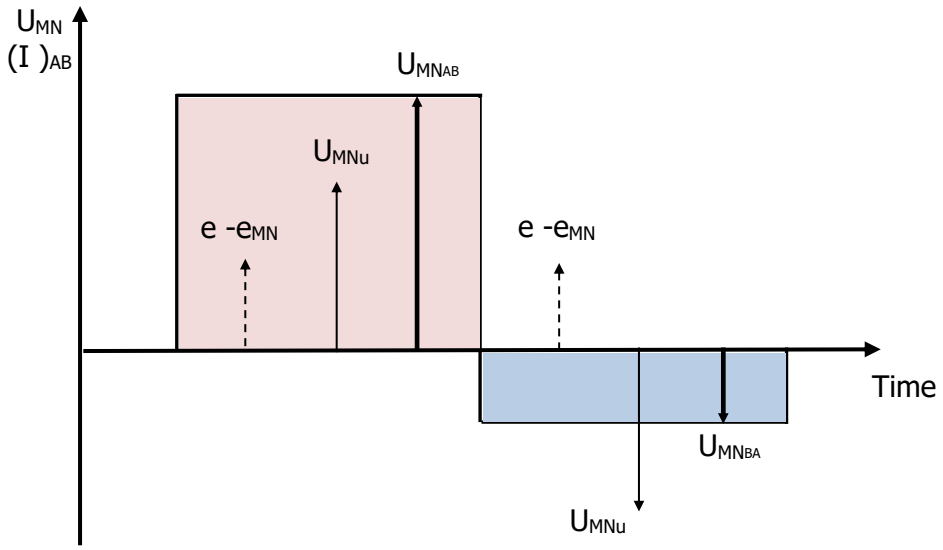

Fig.2.3. *Elimination of electrode polarization difference*

To achieve this goal, an H-bridge with FET transistors powered by the inverter and controlled by pulse trains generated by the microprocessor module is used. The control signals are separated from the microprocessor unit by optocouplers with control signal shapers for FET transistor gates, type TLP250.

2.4 Amplifier for the measurement of the power line current

The signal amplifier for measuring the current strength in the supply electrodes A and B (AMPI) is a Texas Instruments AMC1301 isolation amplifier module, designed specifically for the measurement of a current and gain G=8.2 - Fig.2.5.

The output signal of the module is shifted to +2.5V, which allows its digitization using a unipolar analog-to-digital converter, when the direction of the current in the supply line changes.

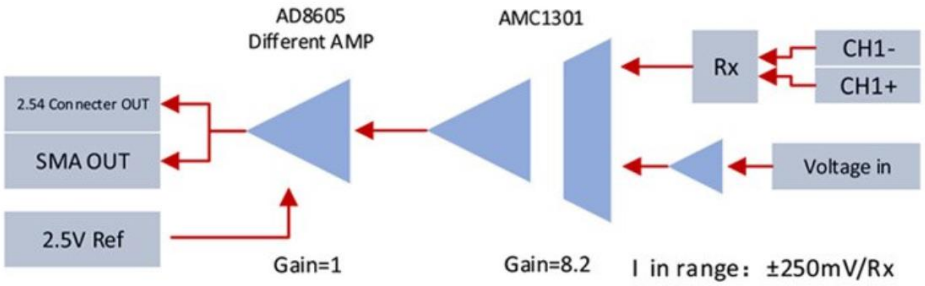

Fig. 2.5. *Amplifier for the measurement of the current in the power line*

The current sensor is a wire resistor with a resistance of 0.2Ω, 2W, 0.1%.

2.5 Voltage amplifier in the receiving line

The choice of a voltage amplifier between the receiving electrodes M and N is important for the stability and accuracy of the received data. This significance is determined by the nature of the input signal - a weak useful signal against a background of comparable and/or much larger interfering signals.

2.5.1 Assessment of the type and amplitudes of the interfering signals

The measurement of the DC and AC components of the interfering signals without current in the power line (AB) was performed using the scheme shown in Fig. 2.6.

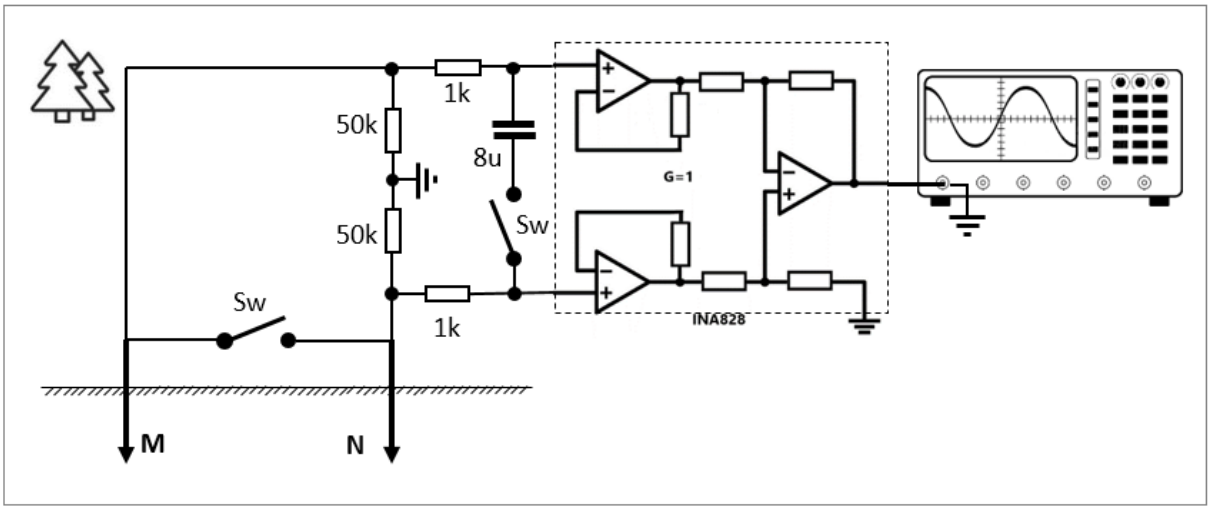

Fig. 2.6. *Circuit for measuring interfering signals without current in the supply line*

Oscillograms recorded at the output of the instrumentation amplifier INA828 with gain G=1 are shown in Fig. 2.7 (a) and (b) - for brass electrodes and (c) and (d) - for stainless steel electrodes. To better analyze the structure of the input signals, the time scales of the corresponding records on the left and right are different. The records presented in Fig. 2.7 (a) and (c) are of 20 s sweep time and show the long-term changes of the input signal, while the records from Fig. 2.7 (b) and (d) have a 50 ms sweep time and show the higher frequency disturbance components. The input protection resistors (1kΩ) together with the capacitor (8uF) form a low-pass filter with a cutoff frequency of about 20 Hz. The attenuation of signals with a frequency of 50 Hz of such a filter is 15dB (5.62 times).

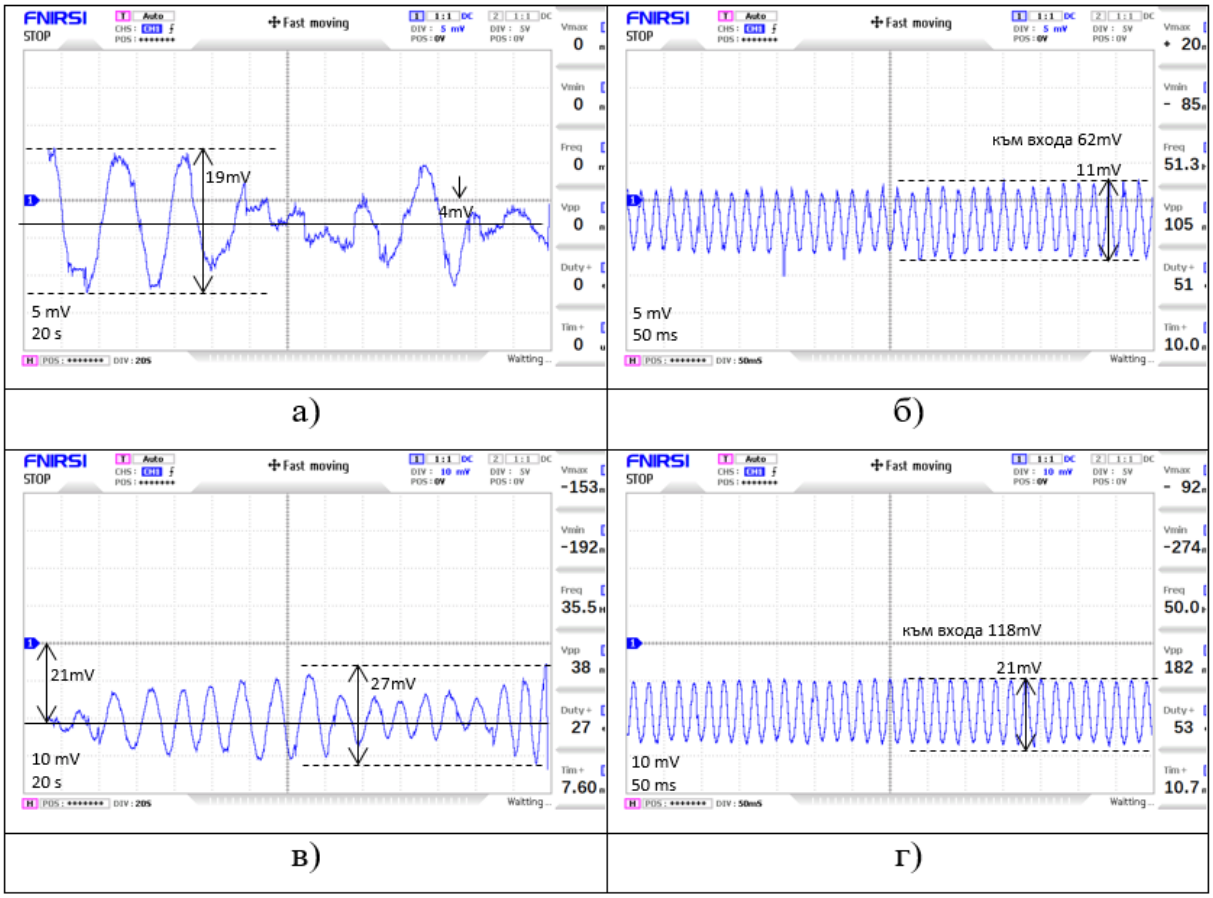

Fig.2.7. *Oscillograms of the interfering signals for brass electrodes a) and (b) and stainless steel electrodes (c) and (d)*

The analysis of the oscillograms presented in Fig. 2.7 gives rise to the following conclusions:

- With both types of electrodes, another ultra-low-frequency component with a frequency of 15-30mHz (T = 66-33s) and a changing amplitude of up to 20-30 mVp-p is superimposed on the expected direct current component as a result of the polarization of the electrodes - fig. 2.7 a) and c). This frequency range is typical of telluric currents caused by geomagnetic storms, so these ultra-low-frequency oscillations are most likely their consequence. For the measurement time (~ 5 - 6 s) they can be taken as a disturbing DC source;
- The direct current component resulting from differences in electrode polarization is about 4mV for brass electrodes and about 20mV for stainless steel ones (5 times larger);
- The interfering AC component with an industrial frequency of 50Hz, fig. 2.7(b) and (d), is of variable amplitude - from 5 mVp-p to 120 mVp-p (adjusted to the input, i.e. taking into account the attenuation from the input RC filter) and is caused by the nearby high-voltage power line.

2.5.2 Estimation of useful signal amplitude

The measurements to estimate the amplitude of the useful signal were carried out with a pulse generator operating with changing polarity, using the measurement setup shown in Fig. 2.8.

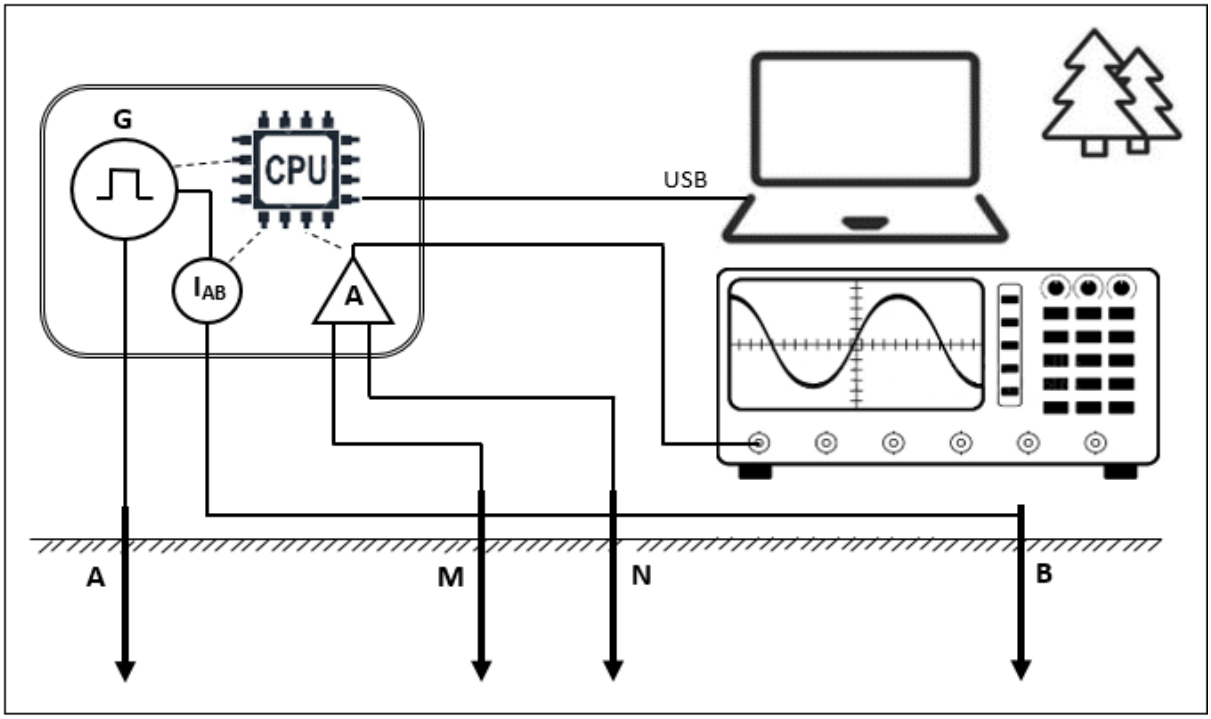

Fig. 2.8. *A scheme for estimation of the useful signal amplitude*

Using the USB interface of a handheld computer, the pulse parameters - duration and target current strength (I_{aim}) in the power line are programmed. On the same interface, the values of the current in the power line A-B and the voltage between the receiving electrodes M-N are obtained.

The amplifier output oscillograms are presented in Fig. 2.9 (a) for brass and (b) for stainless steel electrodes.

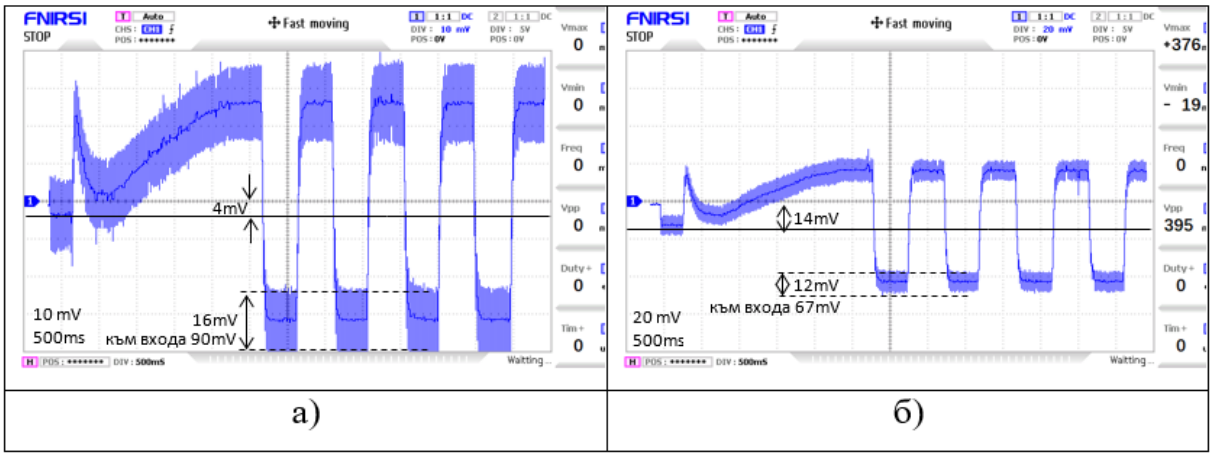

Fig. 2.9. *Oscillograms of the useful signal for brass electrodes a) and stainless steel electrodes b)*

The oscillograms presented in Fig. 2.9 are a reason to draw the following conclusions:

- For the given setup at a current strength of 0.5A, about 15mV useful signal is obtained at both types of electrodes;
- The DC component, due to differences in electrode polarization, is the same as the one with no signal in the supply electrodes;

- After making repeated recordings and comparisons of the output signal from the amplifier over random time periods ranging from 10 to 30s, it became clear that for both the brass (Fig. 2.9 a) and steel electrodes (Fig. 2.9 b) the DC offset did not change with time, i.e. the effect of telluric currents was not observed on the oscillograms in the presence of a signal. This means that they can be represented as a source with high internal resistance working in parallel to the source of the useful signal.

Therefore, for the input signal structure in the receiver it can be summarized that:

1. The useful signal has an amplitude of 15mV (at 500mA current in the supply line);

2. The DC offset is 4mV for brass and 20mV for steel electrodes as a result of the polarization of the electrodes.

3. The AC component (50Hz) is of variable amplitude (10 mV_{p-p} to 120 mV_{p-p}) as a result of industrial disturbances.

4. The interference signal from telluric currents is negligible. But even if some interference voltage from it were to appear, it would not affect the measured value of U_{MN} , since its period is much greater than the time between two successive measurements (when the direction of current in the supply line changes).

2.5.3 Design of the amplifier

After taking into account the parameters of all interfering signals, the necessity of processing bipolar useful signals and the convenience of working with an analog-to-digital converter with a unipolar power supply, the structural scheme of the voltage amplifier at the receiving electrodes, presented in Fig. 2.12, was synthesized.

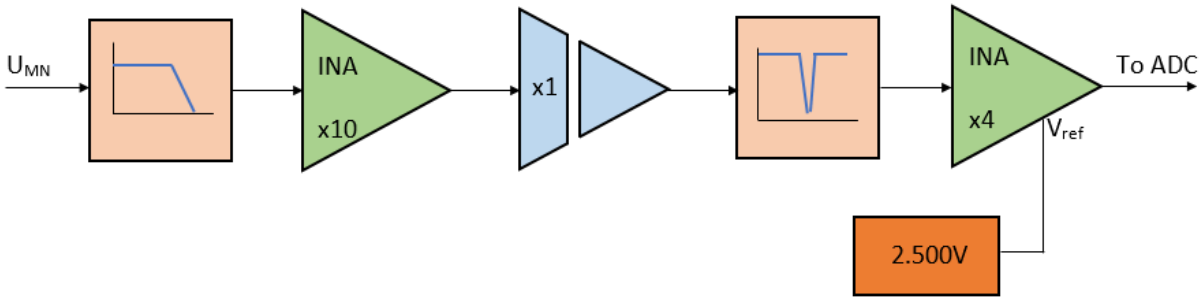

Fig. 2.12. *Structural diagram of the voltage amplifier in the receiving electrodes*

The circuit contains the following blocks: a passive low-pass input filter, an instrumental amplifier with a gain factor of 10, an isolation amplifier with a gain factor of 1, an active cut filter at 50 Hz, a second amplifier with a gain factor of 4 with a level offset of +2.500V.

The scheme of the hardware implementation of the amplifier, together with the amplifier for measuring the current in the supply electrodes, the analog-to-digital converter and the isolated I2C interface to the CPU are shown in (Fig. 2.13).

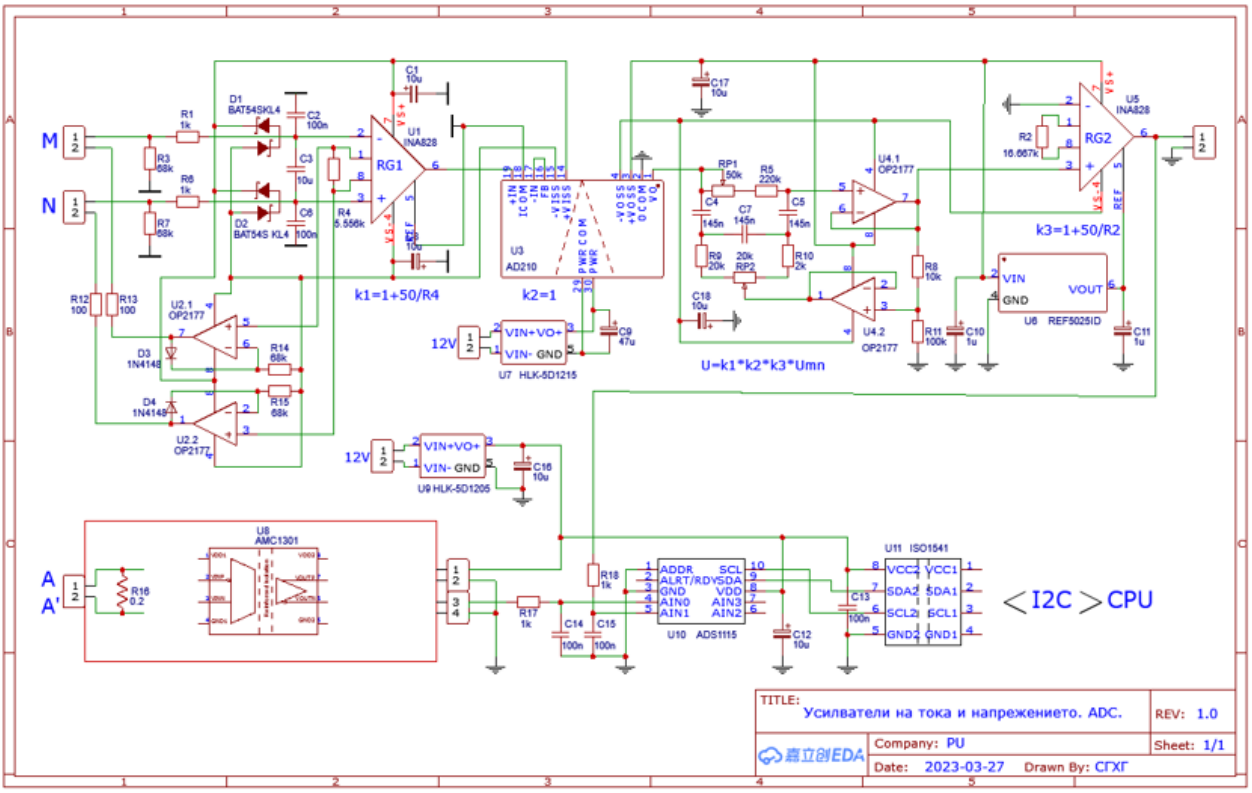

Fig.2.13. *Circuit diagram of the amplifiers for voltage and current measurement, ADC and I2C interface to the CPU*

2.5.4 Scheme simulation

To simulate the operation of the amplifier, a simulation circuit of a voltage amplifier in the receiving line was created and analyzed in the Multisim environment - Fig. 2.16. In it, the useful input signal is simulated by XFG1, the interfering signal from industrial sources and from electrode polarization mismatch - by XGF2, and the interfering signal from telluric currents - by XGF3. The value of the filtering capacitor C_3, determining the time to establish stable voltage values in the receiving electrodes, was optimized by simulation.

In Fig. 2.19, the oscillograms from the simulation (from the left) and those recorded in real conditions (from the right) are shown in parallel, as follows: (a) and (b) - at the input of the instrumental amplifier, (c) and (d) - at its output (before the active rejection filter) and (e) and (f) - at the output of the rejection filter, before the final gain and level shift.

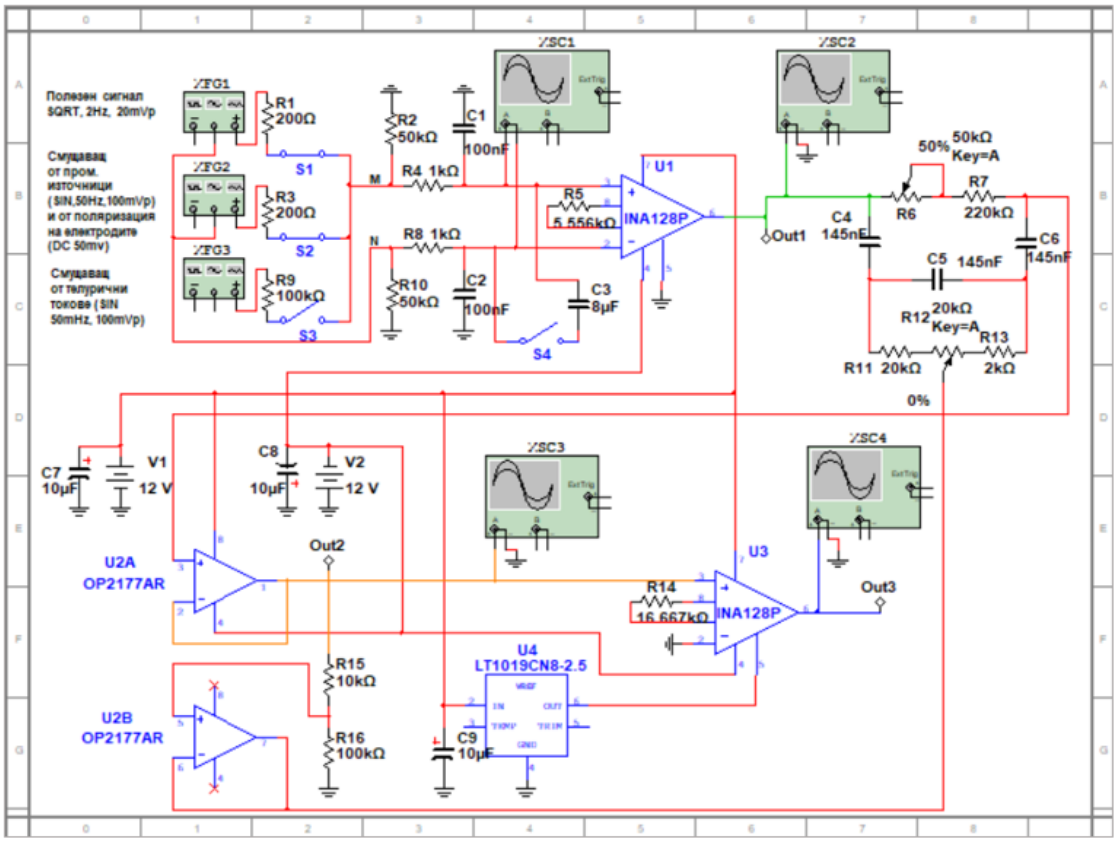

Fig. 2.16. *Simulation circuit of a voltage amplifier in the receiving line*

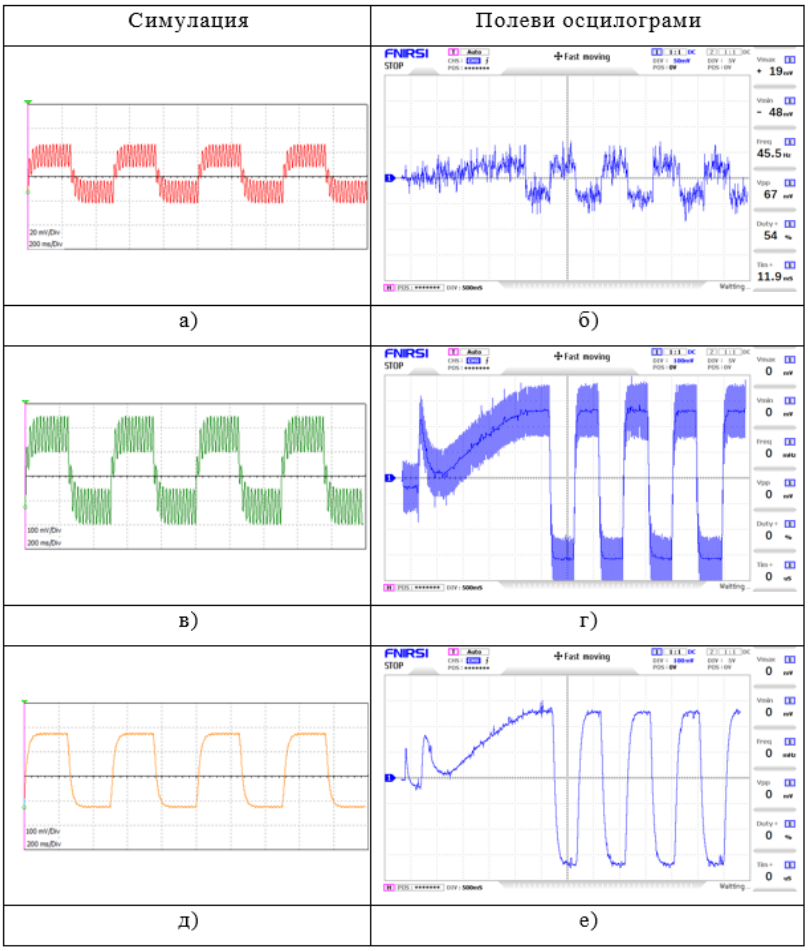

Fig. 2.19. *Comparison of the oscillograms from the simulation - (a), (c) and (e) and field recorded - (b), (d) and (f)*

To determine the working range of currents of the implemented voltage converter (DC-DC inverter), for the chosen place of placement of the electrodes, a test program was compiled to measure the U_{MN} at different values of the current strength in the current electrodes. The results of the measurements are shown in Fig. 2.20. The values of the target current I_{aim} are plotted on the horizontal axis, the values of the reached current I_{AB} on the left vertical axis, and the values of the useful signal in the receiving electrodes on the right vertical axis.

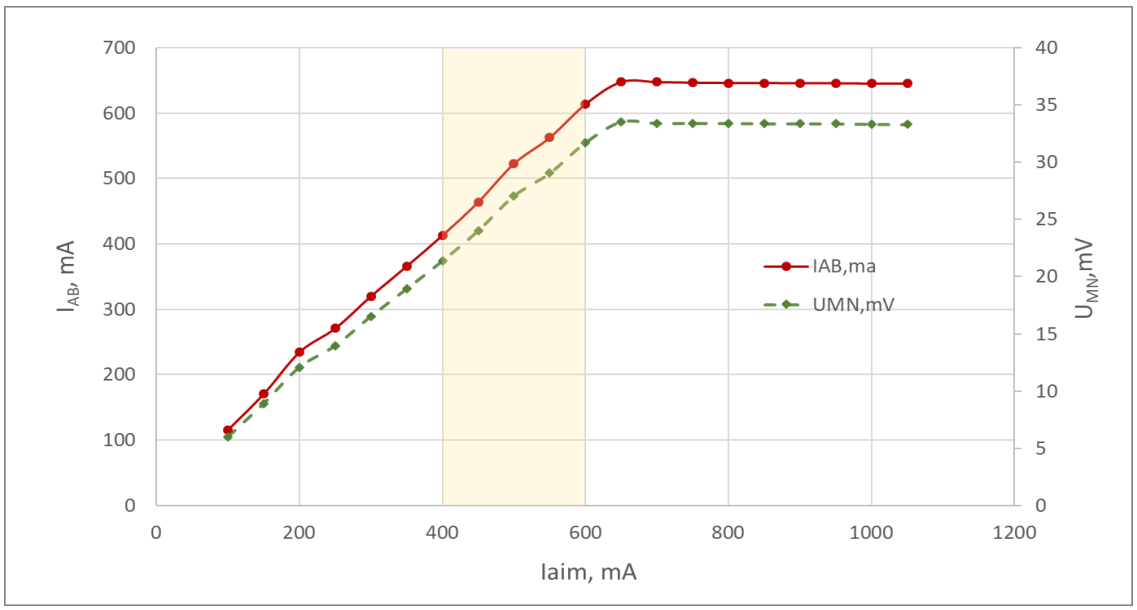

Fig. 2.20. *Determining the operating range of currents*

From the graphs, it can be seen that at the given location, with the specific geometry of the installation (AM=BN=520m, and MN=21.7m) and currents of 100 to 650mA in the supply line, the amplitude of the useful signal is from 5 mVp to 35 mVp. It is obvious that the maximum power of the voltage converter (determined to be about 110W in the laboratory) is insufficient to achieve an operating current above 650 mA. The changes in the apparent resistivity which are supposed to be related to the preparation of earthquakes observed by the author and others and described in item 1.8 of Chapter I, are in the range of 3% to 30%. Therefore, a target operating current (I_{aim}) of around 500mA would be a suitable choice for this installation – large enough to generate a noticeable useful signal and sufficiently smaller than the maximum inverter current for the installation. Fig. 2.21 shows the dependence of the measured voltage in the receiver electrodes on the current from the power supply. From the good match of the experimental points and the regression line, we can conclude about the good accuracy of the measurements - the root mean square deviation of the measured resistance (shown in the labels above the points) is of the order of 0.1%.

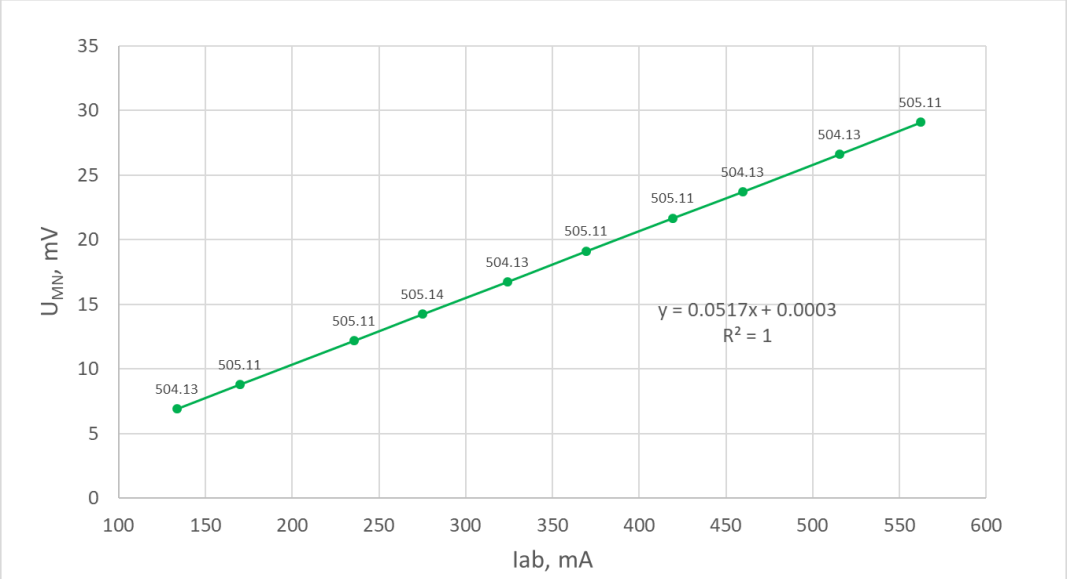

Fig. 2.21. *Dependence of the measured voltage in the receiver electrodes from the current in the current electrodes*

2.6 Analogue to digital converter

This section justifies the need to use an external (to the microprocessor) ADC. A suitable one (ADS1115 from Texas Instruments) is selected and its error is estimated using the worst-case method - 0.02%.

2.7 Calibration, verification and error evaluation

To perform voltage and current calibration, the following scheme has been developed - Fig. 2.23.

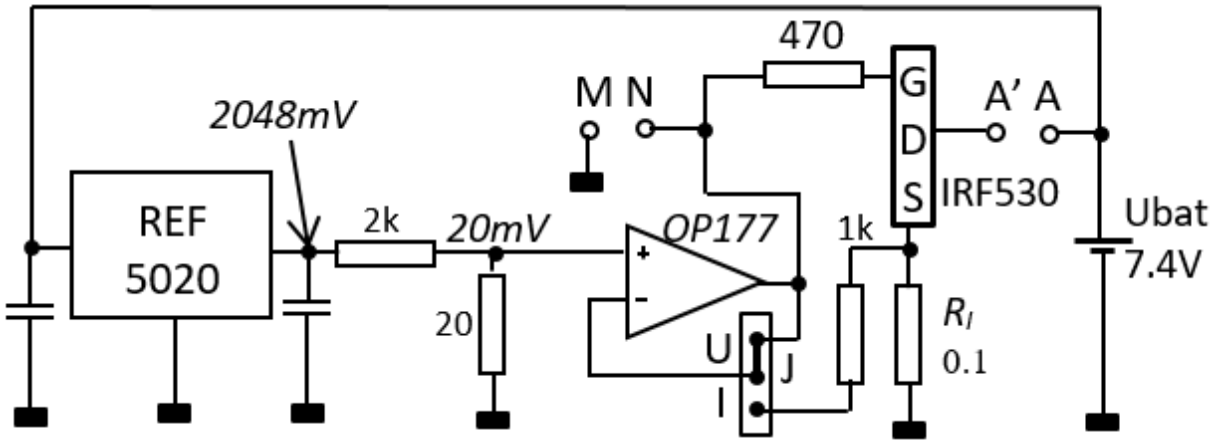

Fig.2.23. *Voltage and current calibration scheme*

The operating mode - voltage or current calibration is selected using the jumper J.

In order to check the operation of the meter in field conditions, the following passive scheme was created - fig. 2.24. Here, R_{AM} and R_{BN} are powerful resistances composed of two series-connected resistances of 150 Ω/10W, and the reference resistance R_{MN} is also wired, 0.100Ω±0.1%, type CP-5 and temperature coefficient 50.10^{-6}/°C.

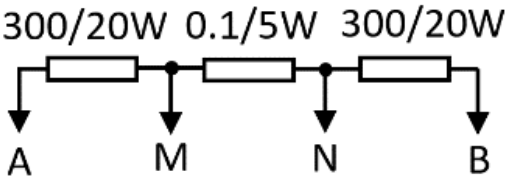

Fig. 2.24. *A scheme of performance and long-term stability check*

The relative uncertainties of the individual voltage and current measurements, as well as that of the calibrator, are used to estimate the error of the geoelectrical resistivity measurement. Thus, a value of 0.374% is obtained for the relative uncertainty of the apparent resistivity meter.

The long-term stability of the apparatus is illustrated in Fig. 2.25. It shows the reference resistance values obtained from the test circuit (100mΩ) over the period of about 15 days during the measurement period.

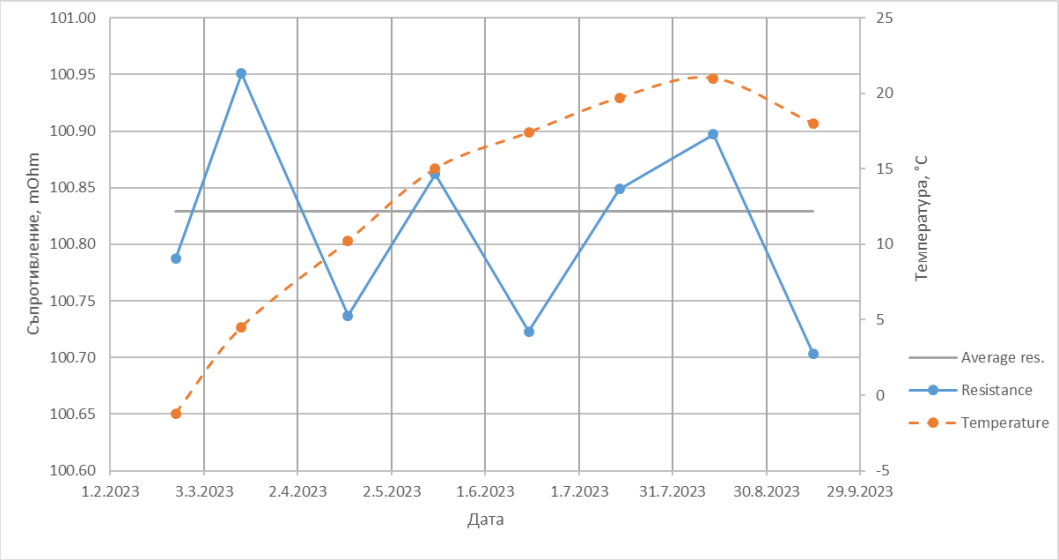

Fig. 2.25. *Long-term stability check*

It shows that the reference resistance measurements from the test circuit differ over time within a standard deviation of 0.1mΩ, i.e. 0.1%., which is within the temperature instability of this resistance 50.10^{-6}/ °C within a temperature range of 20°C.

2.8 Measurement of meteorological parameters

The temperature and humidity of the air as well as the atmospheric pressure are measured using the AHT20 +BMP280 module. The module is mounted in a PVC pipe with a diameter of 26mm, together with the antenna and the LoRa module, and is connected via an I2C bus to the central processor.

A tipping bucket rain gauge, model WH-SP-RG of MISOL, is used to measure the amount of precipitation. To measure the number of tippings, a circuit based on a separate 8-bit AVR microcontroller operating in sleep mode and getting out of it by interruption when a pulse from the precipitation sensor is received or when data for the number of pulses (amount of precipitation) is requested on the I2C bus from the CPU.

2.9 Measurement management

The process of measurement and registration of measurement data is controlled by a microprocessor module with ESP32. To save power, its unused modules are disabled by software, the two LEDs are removed, and the AM1117 voltage regulator is replaced with an AP7361 (with the smaller quiescent current and voltage drop between the input and output, which allows the module to be powered in "sleep" mode from 3.7V battery. Added to the microprocessor module is a real-time module based on DS3231, powered by a Li-Ion battery and controlled by ESP32 via I2C bus. In addition to being transmitted via the LORA module, the data is also saved to an SD card via the added SD Card module, controlled by the ESP32 via the SPI bus.

2.10 Power packs, batteries, solar panel

This paragraph discusses the power management scheme of the individual modules.

CHAPTER III. SOFTWARE CONTROL AND PRACTICAL IMPLEMENTATION OF INSTRUMENTATION FOR MEASURING VARIATIONS OF GEOELECTRICAL RESISTIVITY

3.1 Algorithm of the measurement management program

Fig. 3.3 shows the variation of the direction and value of the current magnitude in the current electrodes over time, together with the time delays and measurement moments (indicated by arrows).

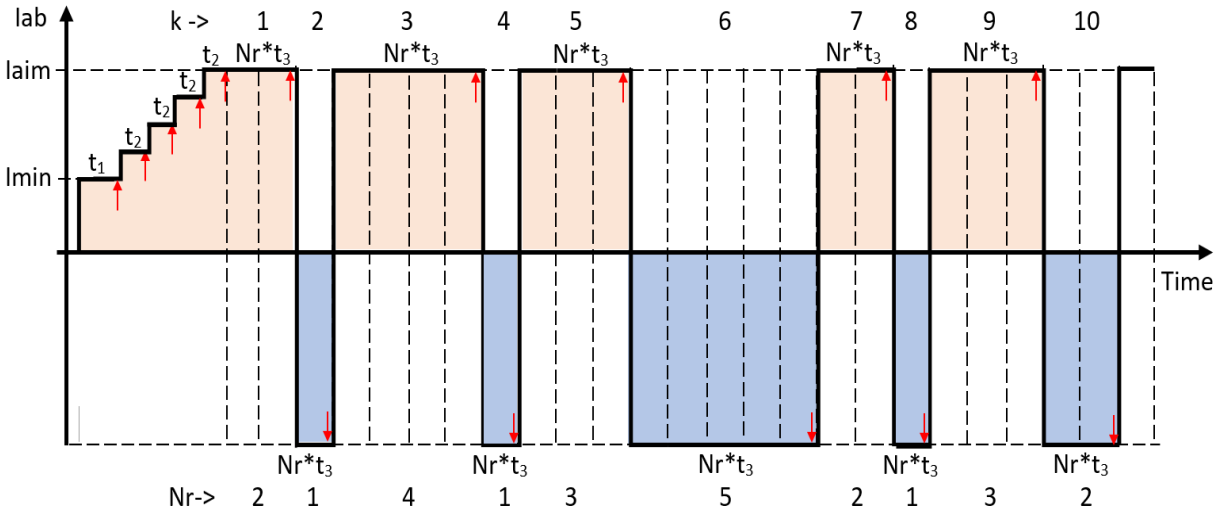

Fig. 3.3. *Time diagrams of the measurements*

In addition, this paragraph describes the algorithm of the measurement control program - Fig. 3.2.

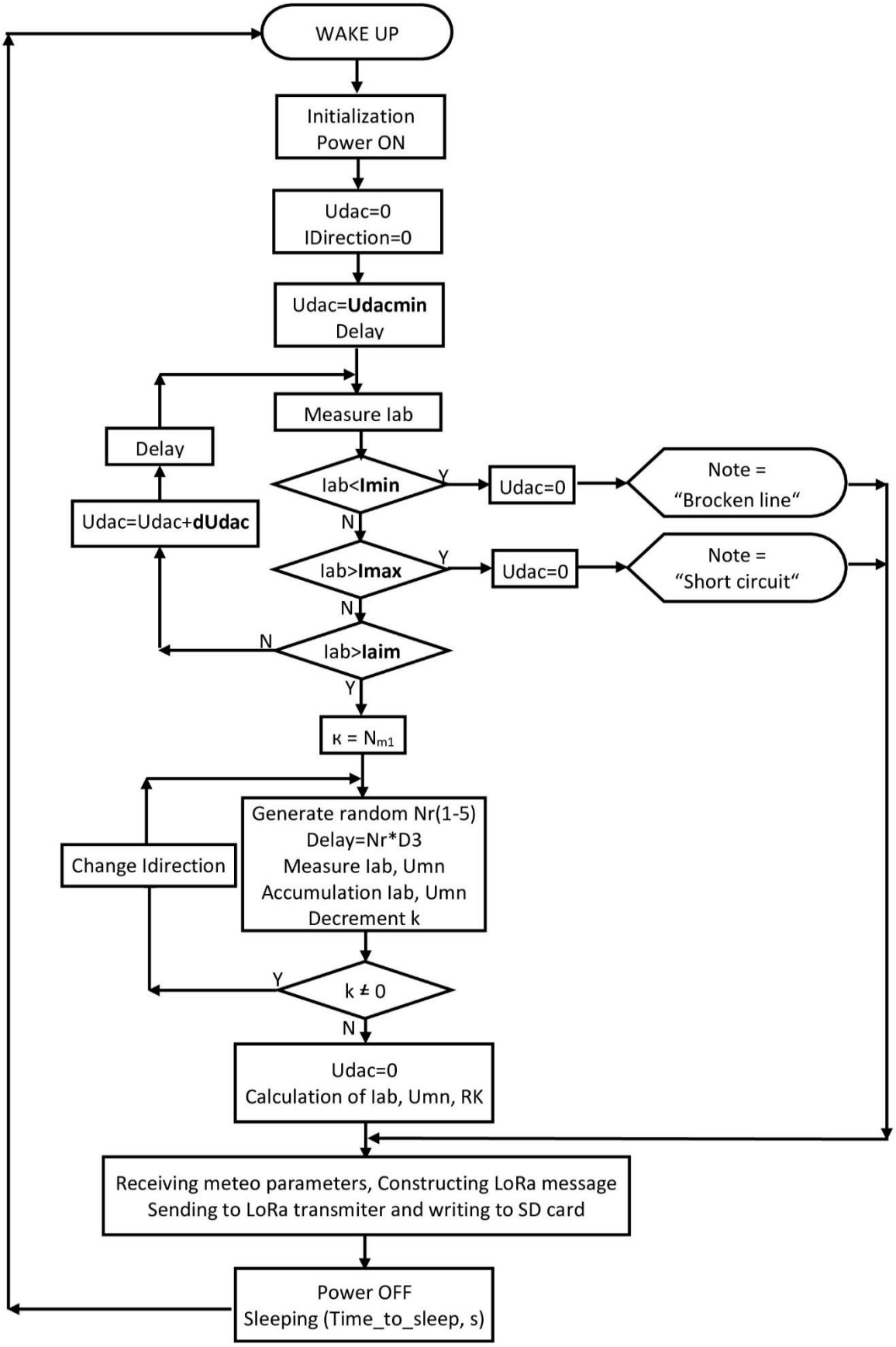

Fig. 3.2. *Algorithm of the measurement management program*

3.2 Practical implementation

Here are shown the developed circuit boards of the individual modules, the internal appearance of the device - Fig. 3.6., the appearance of the electrodes - Fig. 3.11., photographs of the area and the apparatus setup - Fig. 3.12.

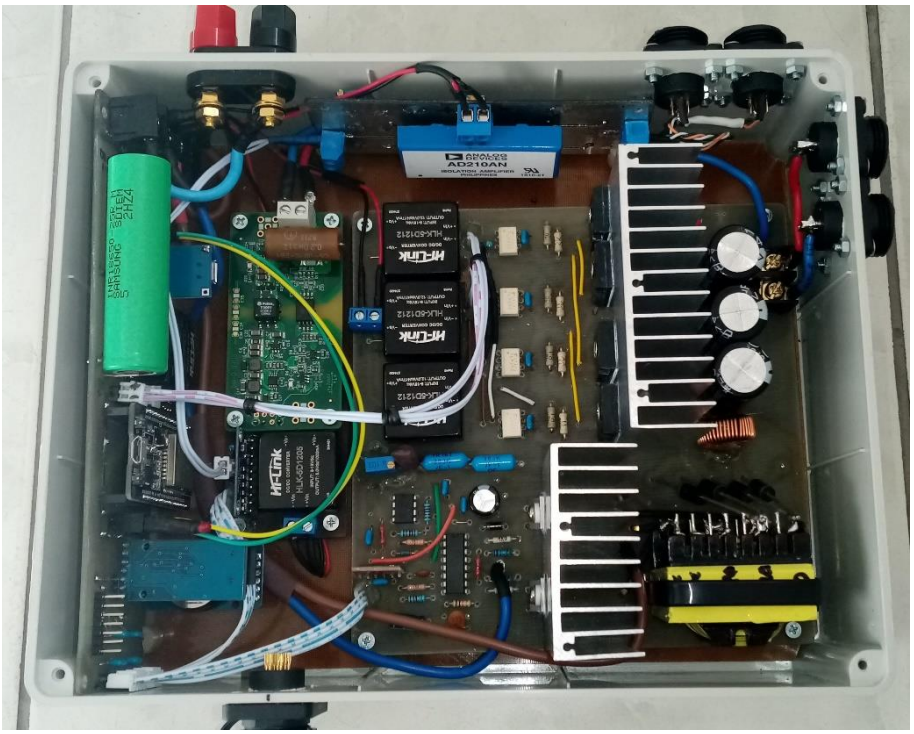

Fig. 3.6. *Internal view of the device*

Fig. 3.11. *Mounted current (A or B) electrode*

Fig. 3.12. *Apparatus setup*

3.3 Results from the observations

This paragraph shows the data on the earthquake activity in the area for the monitored period (from 22.02 to 31.10.2023), according to data from EMSC - Fig. 3.14.

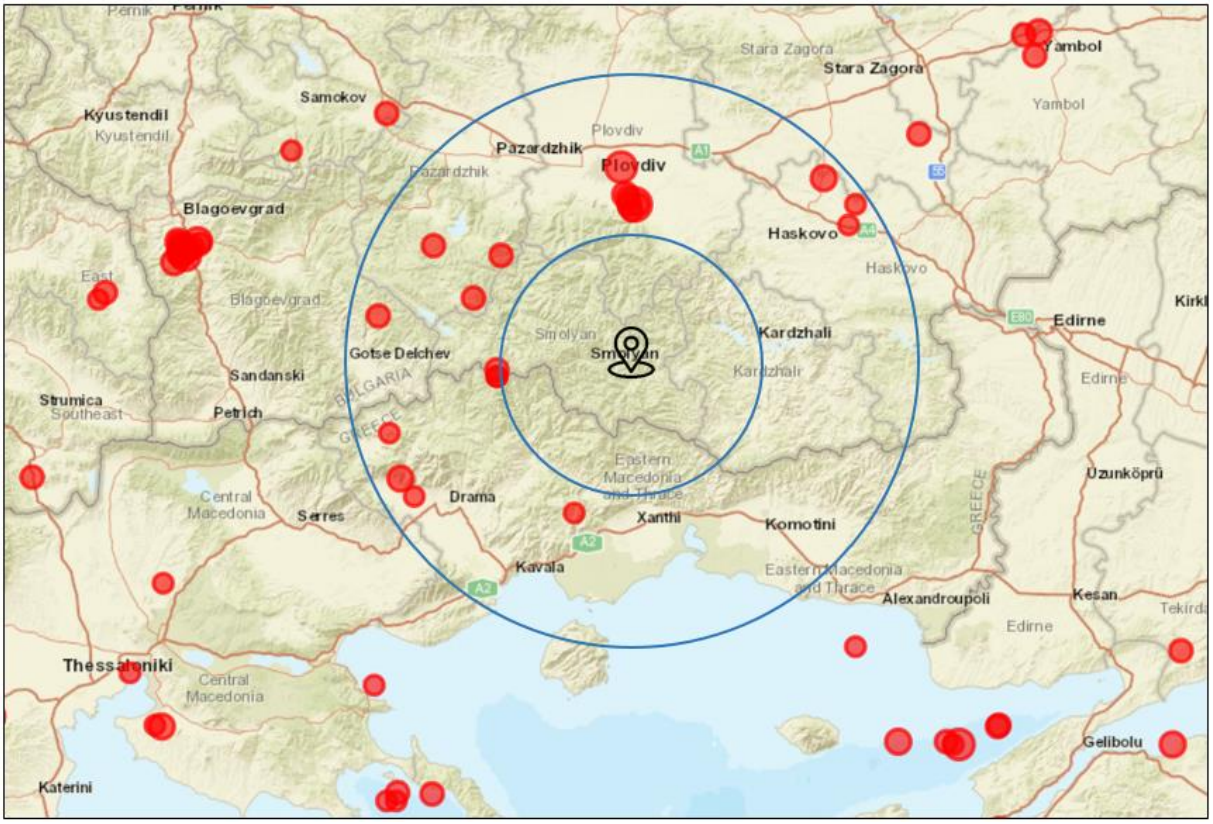

Fig.3.14. *Realised earthquakes in the period of observation*

During the observation period, there were 21 earthquakes with magnitude M ≥ 2.5 and epicentral distances below 100 km.

Fig. 3.15 shows the recorded changes in the apparent resistivity, temperature and precipitation for this period.

The closest earthquakes to the monitoring site are 3, in the area of the village of Kozhari, about 33 km away and magnitudes between 2.5-2.8. The strongest earthquake during the period occurred near the town of Asenovgrad (M = 4.6), 53km away from the place of registration.

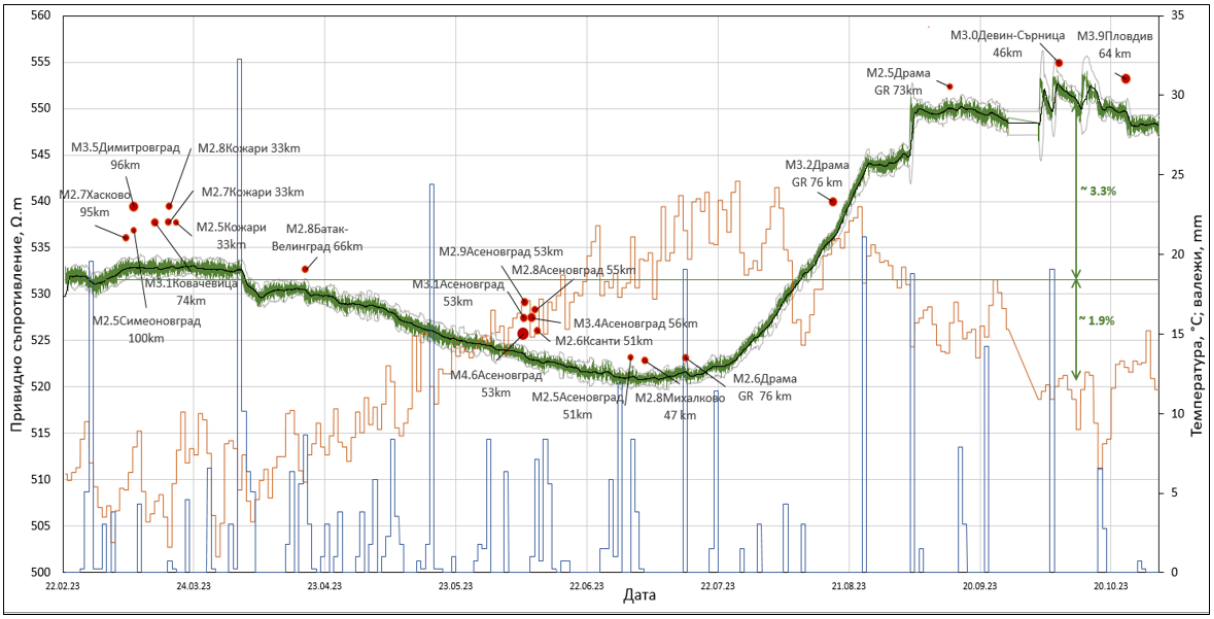

Fig. 3.15. *Changes in geoelectrical resistivity, temperature and precipitation during the observation period*

From this graph we can draw the following conclusions:

1. Changes in the apparent resistance since the beginning of the observation period are from - 2 to +3% and are most likely related to its seasonal changes due to changes in temperature and precipitation.

2. The presumption that the expected changes preceding the earthquakes are larger, as well as the insufficient amount of data, do not allow us to make a connection between the changes in the apparent resistance and the seismic activity.

To determine the influence of temperature and precipitation, correlation coefficients were calculated between daily average values of the apparent resistivity and temperature with lags from 0 to 50 days. The correlation coefficients are negative, and the extreme (-0.954) is at a delay of 22 days - fig.3.17.

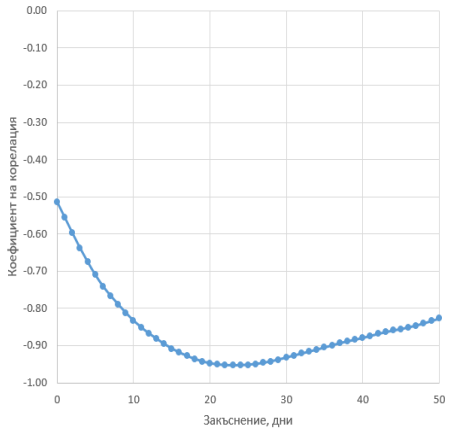

Fig. 3.17. *Extremum of the cross-correlation coefficients between the apparent resistivity and temperature*

No correlation of the apparent resistance with the amount of precipitation is observed - the correlation coefficients are below 0.15.

The relatively long summer drought (22.07 - 24.08) created conditions for studying the influence of soil moisture around the electrodes on the obtained results. Wetting the soil around the current electrodes resulted in a decrease of the apparent resistance Ra by 0.1%, which is within the measurement error - fig. 3.18 (point 1). Wetting the soil around the receiving electrodes, however, led to a sudden increase in the apparent resistance by 0.7% (moment 2), which is relatively high. This confirmed the need for periodic water saturation of the soil around the electrodes (receiving and current) during summer droughts to normalize their contact resistance.

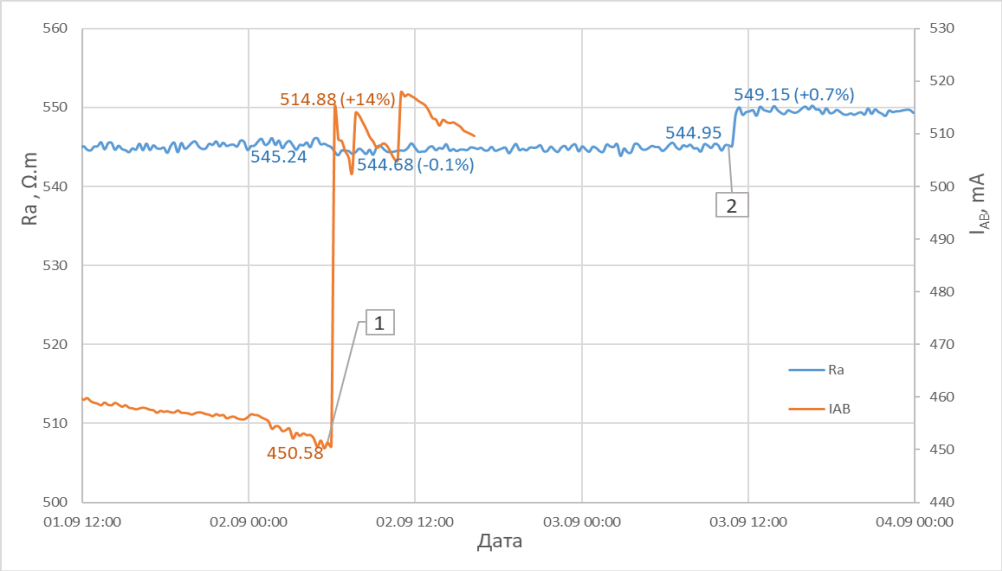

Fig. 3.18. *Influence of the reduction of the contact resistance of the current (moment1) and receiving (moment2) electrodes*

CHAPTER IV. TRANSMISSION AND VISUALISATION OF MEASUREMENT DATA

4.1 Introduction

When designing the system for data transmission and visualization, two approaches were discussed - creating a LoRaWAN network and using IoT platform Thingspeak.

4.2 Overview of the LoRaWAN protocol

This paragraph discusses the network architecture of the protocol, the LoRa modulation used in the physical layer, the structure of the packet in it, the classes of end devices, the mechanisms for ensuring reliable communication and for joining the end devices to the network as well as the LoRaWAN servers.

Fig. 4.6 shows an overview of the LoRaWAN system for acquiring data from earthquake precursors monitoring polygons.

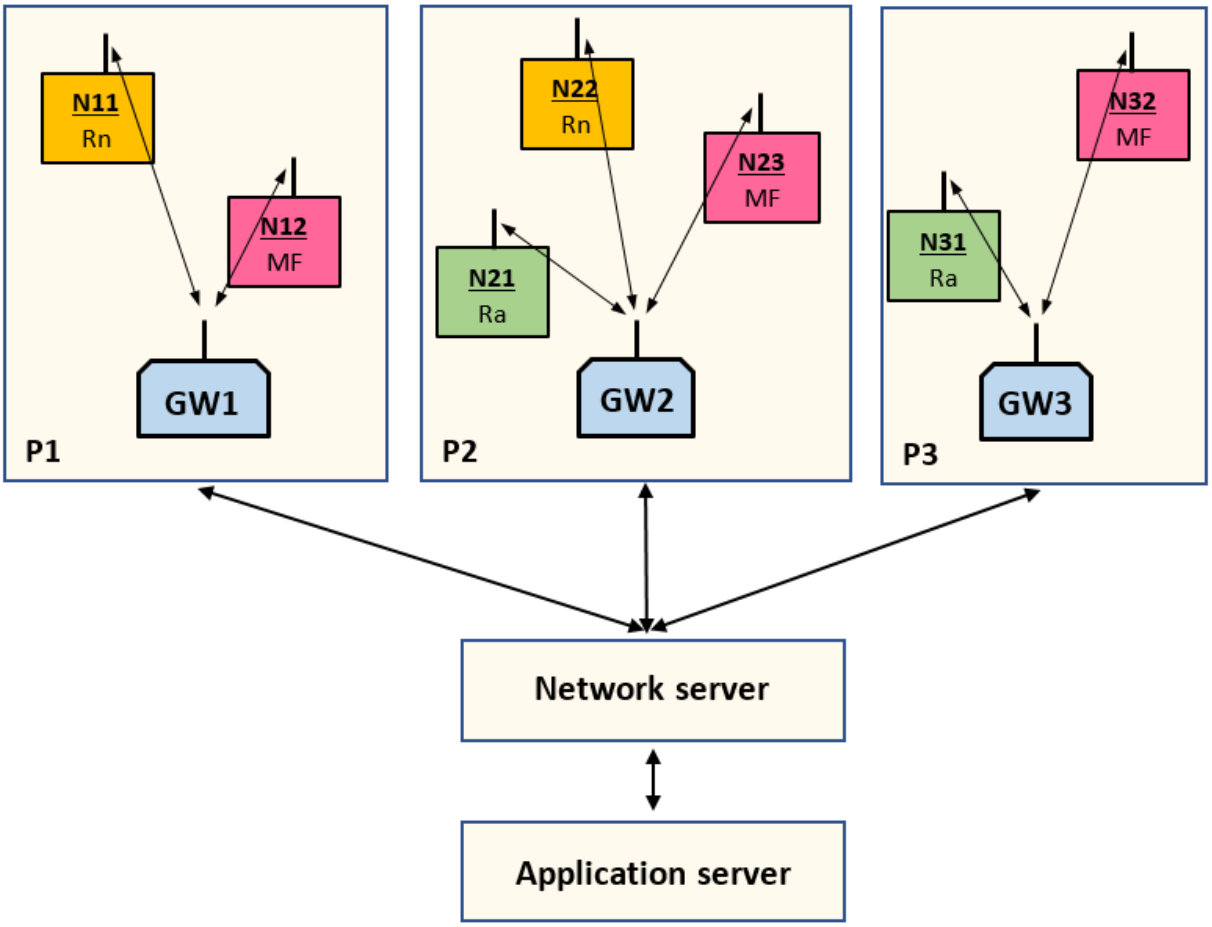

Fig. 4.6. *General plan of a LoRaWAN system for obtaining data from three polygons for monitoring earthquake precursors*

Here P1, P2 and P3 denote the polygons, GW1, GW2 and GW3 – the concentrators for the corresponding polygon, N11-N32 are the individual nodes to which the sensors are connected, e.g. for radon (Rn), magnetic fields (MF), Ra (apparent resistivity and meteorological parameters). If within a polygon the distance between a given node and the concentrator is large, additional repeaters or concentrators can be placed.

4.3 ThingSpeak Platform Overview

General characteristics, methods of reading and writing data to channels, ensuring security, data processing applications and interactions between them, and limitations of the free license for non-commercial use are discussed.

4.4 Selection and implementation of a concept for data transmission, processing, visualization and storage

Given that:

- The design of a LoRaWAN network must be tailored to the specific configuration of the end devices and the terrain topology;
- The current availability of only one final device - the one for measuring the geoelectrical resistance;
- The complexity of developing and maintaining own LoRa servers;
- The high cost of LoRa concentrators and the unreliability of using popular LoRa servers,

to fulfil the tasks that had been set, when choosing a system for data registration, processing and visualization, an intermediate option was designed - using LoRa modulation to transmit the data from the end device to a simple microcontroller, which forms and sends the data packets in Thingspeak channels.

This solution has the following advantages:

- allows for accumulation, processing and visualization of data from geoelectrical resistance measurements without setting up LoRa and Application servers;
- allows the running of an automatic IoT analysis based on events or schedules;
- the speed of receiving the data allows for the use of a free license;
- the price of the microcontroller (sending the data to Tingspeak) is significantly lower compared to that of a LoRa concentrator;
- the use of a LoRa communication module in the end devices will facilitate a future transition to LoRaWAN when their number increases and the purchase of a LoRa concentrator.

The proposed data acquisition, processing and visualization scheme is shown in Fig. 4.8.

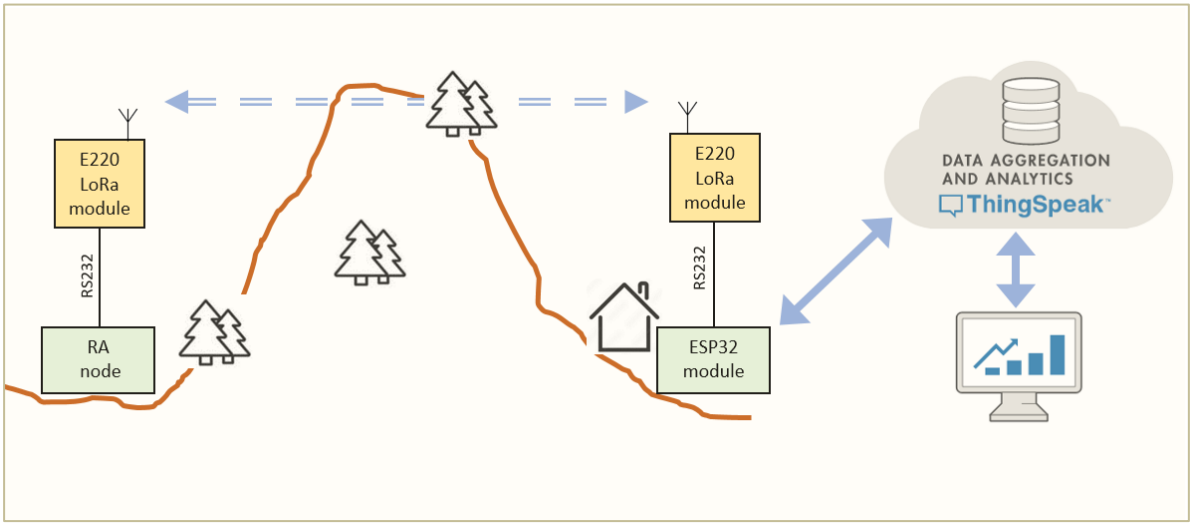

Fig. 4.8. *A scheme of the adopted concept for transmission, processing and visualisation of data from the apparent resistivity measurement equipment*

The choice of Ebyte's E220 LoRa transceiver is further justified. Its advantages and modes of operation are described.

The connection diagram of the two LoRa modules, to the microcontroller of the end device - ESP32(1) and to the device communicating with Thingspeak - ESP32(2) is shown in Fig. 4.10.

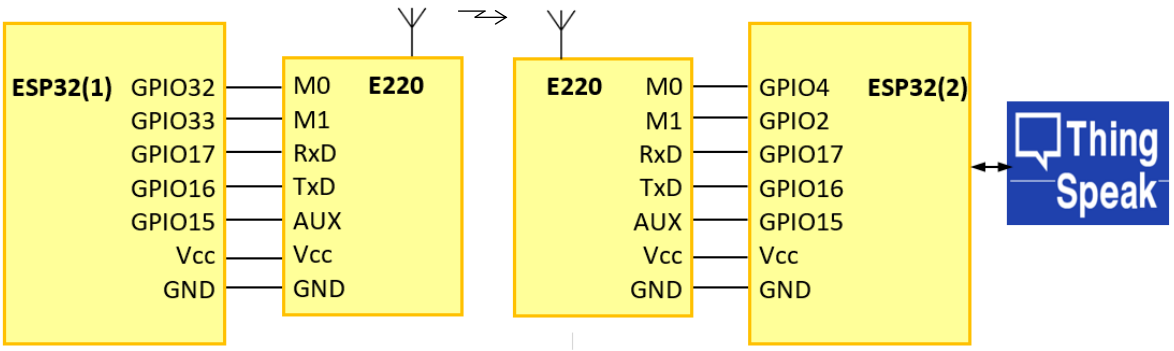

Fig. 4.10. *Connection diagram of the LoRa modules to the microcontrollers*

CONCLUSION

The present dissertation is related to earthquake forecasting research and, in particular, to the registration of one of the established prognostic effects – the change in the electrical resistance of the earth's crust in the process of earthquake preparation.

Chapter one of the dissertation emphasizes the relevance of the problem of obtaining data on the behavior of the earth's electrical resistance before and during earthquakes. A study of the accumulated experience in recording the changes of geoelectrical resistance in connection with the preparation of earthquakes is carried out.

The existing methods and equipment for its measurement are reviewed.

The possible sources of noise and ways to reduce them are analyzed.

An analysis of the results of the observations of apparent resistivity variations in the process of earthquake preparation is made.

At the end of the first chapter, the purpose and tasks of the dissertation work are formulated.

In the **second chapter** of the dissertation, an apparatus for measuring the variations of the geoelectrical resistance is designed.

The nature of the disturbing signals is determined. Their amplitudes are evaluated, relative to the amplitude of the useful signal at the specific geometry of the installation and power of the current source in the supply line.

A simulation study of the voltage amplifier for the receiving line at different amplitudes of interfering signals and at different values of the input filter capacitor is performed in the Multisim environment. The frequency response of the amplifier path is simulated.

The simulation and the actually obtained oscillograms of the signals before and after their amplification are applied and analyzed.

Calibration and verification modules are designed and implemented. An estimate of the error from the geoelectric resistivity measurements is made.

A separate module for measuring meteorological parameters is designed.

The apparatus for measuring the variations of the geoelectrical resistance is realized following the latest innovative achievements of receiving, processing, transmission and registration of sensor data.

The **third chapter** of the dissertation describes the hardware implementation of the apparatus for measuring the variations of the geoelectrical resistance and measuring

meteorological parameters. The first results of its work are shown.

The equipment is installed in the area of the village of Dunevo, Smolyan region.

The operation algorithm of the microcontroller program controlling the measurements is explained. Fragments of the software code are shown.

Data is transmitted using a LoRa module to a base station.

The data obtained from the registration of the geoelectrical resistance and meteorological parameters for a seven-month period are shown together with the realized earthquakes with a magnitude greater than 2.5 and epicentral distances up to 100 km from the installation. An algorithm is described for removing outliers and smoothening the raw data. A cross-correlation is performed with temperature and precipitation.

The influence of drought on the contact resistance of the electrodes, and hence on the magnitude of the operating current and the measured geoelectrical resistance, is investigated.

The amount of data that was obtained is insufficient for deriving a relationship between the variations of the geoelectrical resistance and the realized earthquakes during the observation period.

In the **fourth chapter** of the dissertation, two possible options for the implementation of the transmission, storage and visualization of the data that was received from the equipment for measuring the geoelectrical resistance are considered. The choice of one of them is justified, while the second one, being more expensive and labor-intensive, is postponed for implementation after increasing the number of observed precursors and merging them into polygons.

Appropriate modules are selected and programmed to transfer the data from the field part of the equipment to a Thingspeak channel – a cloud platform with the ability to store, process and visualize the received data.

A MATLAB program is written to process the data and run automatically.

HTML code is also written on a WEB page for visualization of the data from the station in real-time. The page is uploaded to a free WEB domain.

- - - - - - - - -

The ability to predict earthquakes has important social and economic significance.

The conclusion that prevails is that the prediction of earthquakes should be short-term, based on observed physical phenomena. According to some authors, the main reason for the lack of success in the other countries, besides the ambiguity of the precursors, is the concentration of most of the financial and human resources in strengthening the seismographic networks, which are usually not effective in detecting precursors, since many of the precursors are not seismic.

The area around and in Bulgaria is heavily affected by earthquakes and other geodynamic disasters. However, our country lacks a National Earthquake Prediction Project.

The improvement of the instrumental networks connected to modern communication networks is a necessary condition for the successful development of the area and the measurements for seismic protection and forecasting. A solution to this task is the creation of a broad collaboration between scientists from the region of the Balkan countries for seismological, building-structural, preventive, and predictive research. The development of seismology, earthquake engineering, protection and prevention of people is a government task, and government institutions should support research by funding it from various sources and creating conditions for it to be carried out.

CONTRIBUTIONS OF THE DISSERTATION

Scientific and applied contributions:

1. Existing methods, techniques and tools in the field of recording geoelectrical resistivity changes in relation to earthquake preparation are investigated and systematized.

2. Possible sources of noise, ways to reduce them and results of observations of apparent resistivity variations in the process of earthquake preparation are analyzed.

3. The anomaly recorded by the author during the measurement of apparent resistivity in the area of the town of Strazhitsa after the destructive earthquake of 07.12.1986 (M=5.7) is shown and analyzed. It is assumed that the observed anomaly (~14%) preceding the largest (for the period of observation) aftershock, that of 11.05.1987 (M=3.6), is related to seismic activity.

4. The influence of drought on the contact resistance of the electrodes, respectively on the value of the operating current and the measured geoelectrical resistance is investigated. Cross-correlation with temperature and amount of precipitation was performed.

Applied contributions:

1. Equipment for measuring the variations of geoelectrical resistance and meteorological parameters is designed and implemented in hardware. It is installed in the area of the village of Dunevo, Smolyan region.

2. Modules for calibration and verification of the equipment for measuring variations of the geoelectrical resistance are implemented. An estimate of the error of the measurements is made.

3. Data obtained from the registration of geoelectrical resistivity and meteorological parameters over an eight-month period are presented, along with recorded earthquakes with magnitudes greater than 2.5 on the Richter scale and epicentral distances up to 100 km. An algorithm for removing outliers and smoothing the "raw" data is described.

4. Software capability for registration, transmission, processing, storage, and visualization of the received sensor data in a cloud platform is implemented. A program in MATLAB environment has been created to process the station data and visualize them in real-time.

LIST OF PUBLICATIONS RELATED TO THE DISSERTATION WORK

1. Svetoslav Hadzhigenchev, Slavi Lyubomirov. Instrumentation for measuring variations of earth electrical resistivity. Proceedings of the National Scientific Conference with International Participation "Education, Science, Society", Sofia. Paisii Hilendarski University Press, pp. 1092- 1107, ISBN 978-619-7663-43-3 (online), 2022.

2. Svetoslav Hadzhigenchev. Registration of changes in the earth's electrical resistivity in the area of seismic station "Rozhen" (RZN), South Bulgaria. Third National Scientific Conference "Man and the Universe", Union of Scientists in Bulgaria - Smolyan, 25-26 November 2021, Scientific Proceedings of the Union of Scientists in Bulgaria - Smolyan. Volume 3, Part 3, ISSN:1314-9490 (online), pp.631-636, 2022;

3. Svetoslav Hadzhigenchev. Changes of apparent resistivity in the region of Strazhitsa after the earthquakes in 1986. Scientific Proceedings of the Union of Scientists in Bulgaria - Plovdiv. Series B. Technique and technology. Volume XX, ISSN 1311-9419 (Print); ISSN 2534-9384 (Online), pp. 31-35, 2022.

4. Svetoslav Hadzhigenchev. System for continuous monitoring of environmental noise. Scientific Proceedings of the Union of Scientists in Bulgaria - Plovdiv. Series B. Techniques and technologies. Volume XX, ISSN 1311-9419 (Print); ISSN 2534-9384 (Online), pp. 24-30, 2022.

5. Svetoslav Hadzhigenchev. Radon monitor calibration chamber. Scientific Proceedings of the Union of Scientists in Bulgaria - Plovdiv. Series B. Techniques and technologies. Volume XIX, ISSN: 1311-9419 (Print); ISSN 2534-9384 (Online), pp. 66-72, 2021.